

# An almost head-on collision as the origin of two off-centre rings in the Andromeda galaxy

D.L. Block<sup>1</sup>, F. Bournaud<sup>2,3</sup>, F. Combes<sup>2</sup>, R. Groess<sup>1</sup>, P. Barmby<sup>4</sup>, M.L.N. Ashby<sup>4</sup>, G.G. Fazio<sup>4</sup>,  
M.A. Pahre<sup>4</sup>, S.P. Willner<sup>4</sup>

<sup>1</sup> Anglo American Cosmic Dust Laboratory, School of Computational and Applied Mathematics, University of the Witwatersrand, Private Bag 3, WITS 2050, South Africa

<sup>2</sup> Observatoire de Paris, LERMA, 61 Av. de l'Observatoire, F-75014, Paris, France

<sup>3</sup> Present Adress: DSM/DAPNIA/Service d'Astrophysique, CEA/Saclay, 91191 Gif-sur-Yvette Cedex, France

<sup>4</sup> Harvard-Smithsonian Center for Astrophysics, 60 Garden Street, Cambridge, Massachusetts

Received 24 May 2006 ; Accepted 18 August 2006 ; Published in Nature, October 19th issue.

**Abstract.** The unusual morphology of the Andromeda Spiral (Messier 31, the closest spiral galaxy to the Milky Way) has long been an enigma. Although regarded for decades as showing little evidence of a violent history, M 31 has a well-known outer ring<sup>1-7</sup> of star formation at a radius of 10 kpc whose center is offset from the galaxy nucleus. In addition, the outer galaxy disk is warped as seen at both optical<sup>8</sup> and radio<sup>9</sup> wavelengths. The halo contains numerous loops and ripples. Here we report the discovery, based on analysis of previously-obtained data<sup>10</sup>, of a second, inner dust ring with projected dimensions 1.5 by 1 kpc and offset by  $\sim 0.5$  kpc from the center of the galaxy. The two rings appear to be density waves propagating in the disk. Numerical simulations offer a completely new interpretation for the morphology of M 31: both rings result from a companion galaxy plunging head-on through the center of the disk of M 31. The most likely interloper is M 32. Head-on collisions between galaxies are rare, but it appears nonetheless that one took place 210 million years ago in our Local Group of galaxies.

Newly-acquired images<sup>10</sup> of M 31 secured by the Infrared Array Camera<sup>11</sup> (IRAC) onboard the Spitzer Space Telescope span the wavelength regime of 3.6 to 8.0 microns. These images offer unique probes of the morphologies of the stellar distribution and interstellar medium with no interference from extinction. Figure 1 shows the emission map of the interstellar medium at 8 microns, generated by subtracting a scaled 3.6 micron image (dominated by starlight) from the 8 micron image. The subtraction removes the contribution from stellar photospheres and leaves only the emission from dust grains<sup>10</sup>, which trace the interstellar medium of M 31. What is most striking in Figure 1 (and in the enlarged inset) is the presence of a complete though asymmetric inner ring of dust 6.9 by 4.4 arcmin in extent, translating to linear dimensions of about 1.5 by 1 kpc (assuming a distance<sup>12</sup> of 780 kpc). The inner ring lies between the two well known Baade spiral dust arms<sup>13</sup>, both of which are clearly seen in emission. The inner ring is elongated in a direction close to the minor axis and belongs to the central gas disk, which appears to be more face-on<sup>14</sup>. It is therefore not possible to know the inner rings precise ellipticity, but it is unlikely to be circular. IRAC imaging thus reveals two rings. The outer ring is offset by approximately 10 percent of its radius, while the inner ring is offset by about 40 percent or 0.5 kpc. The inner elliptical ring has been alluded to in earlier studies<sup>15,16</sup>, but all investigators have hitherto believed it to be a mini-spiral, related to a bar. Published Spitzer 24 micron images<sup>5</sup> of M 31 show centrally-concentrated dust emission; the ring morphology is therefore disguised at these longer wavelengths. The IRAC images beautifully show the inner ring at high spatial resolution and furthermore confirm that this feature is a complete and continuous ring, even though offset and asymmetrical. There are two known scenarios whereby disk systems form rings: by head-on galaxy collisions or by rotating bars. Head-on collisions differ from common tidal interactions between galaxies because the pericentric distance of the orbit of the companion is small and its orbit is almost perpendicular to the target disk. Such collisions produce expanding ring-shaped waves<sup>17</sup>. Rotating bars in spiral disks produce inner, outer, and sometimes nuclear rings in barred spiral galaxies. The rings occur at orbital resonances and arise from the galaxy's internal dynamics (unlike collisional rings). Many examples of bar-induced rings are known<sup>18</sup>.

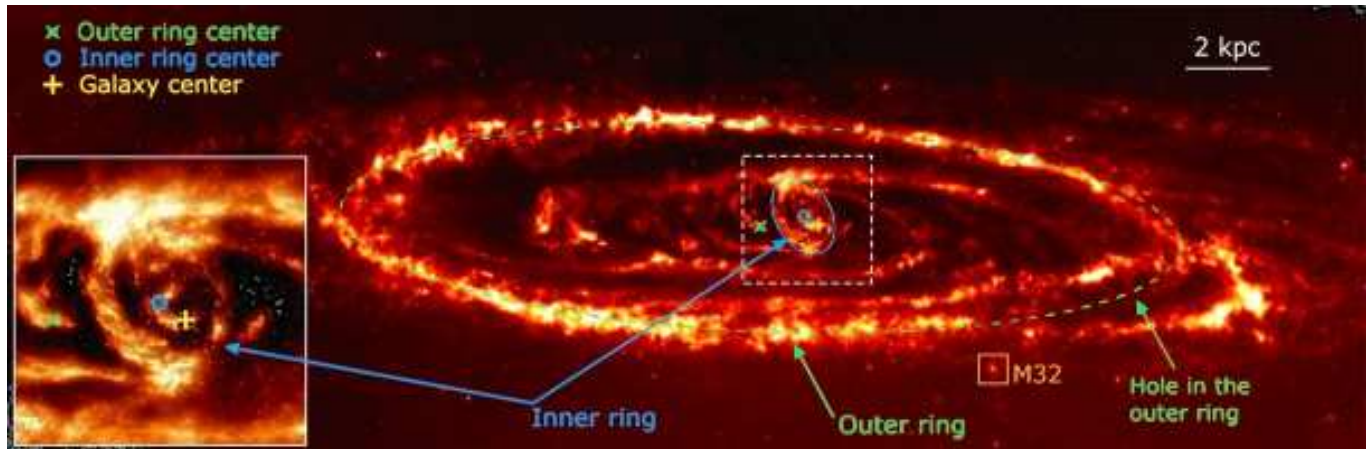


**Fig. 1.** The Andromeda Galaxy M 31 observed with the Infrared Array Camera<sup>11</sup> on board the Spitzer Space Telescope at a wavelength of 8 microns. A scaled version of the 3.6 micron image was subtracted from the 8 microns image to remove light from stellar photospheres. The remaining emission therefore traces the emission of warm dust grains and macromolecules in the interstellar medium. M 31 clearly possesses two rings. Apart from the famous outer dust ring seen at a radius of 10 kpc, this map reveals a second 1.5 by 1 kpc inner dust ring offset by approximately 0.5 kpc from the galaxy nucleus. Both rings are interpreted to be density waves induced by an almost head-on collision. The most likely candidate is the dwarf companion galaxy M 32, which appears faint in this image because it has little dust. The starlight of M 32 is however prominent in the separate 3.6 and 8 micron images.

Infrared imaging of spiral galaxies in the Local Universe confirms the ubiquity of the bar phenomenon; about 80% of spiral galaxies are barred<sup>19</sup>, even if many are classified as unbarred at visible wavelengths. M 31 is no exception; although Hubble classified it as normal type Sb, it is likely to possess a stellar bar. The presence of a bar in M 31 is suggested by its boxy bulge, which is conspicuous in infrared imaging<sup>5,20</sup> and is aligned almost parallel to the galaxy's major axis. The boxy bulge might be an inflated bar, or it may hide a thinner parallel bar (at about 10 degrees from the major axis). There is, however, no bar parallel to the minor axis, along which the major axis of the inner dust ring lies. Had there been a stellar bar along the minor axis, it would surely have been detected in the IRAC 3.6 micron image<sup>10</sup>, which is much deeper than the 2.2 micron 2MASS images and less affected by dust attenuation. The double-ring system of M 31 therefore appears unrelated to any possible central bar, because the elliptical inner ring does not have the typical orientation of most bar-induced gas rings (generally aligned along the bar's major axis). Moreover, the off-center ring strongly supports the collision interpretation. Resonant rings generated from rotating bars are rarely as off-center as the rings of M 31, and the amount to which such rings show an off-center increases with radius. In M 31, however, the inner ring is off-center by 40% of its radius whereas the outer ring is off-center by only 10%.

The relative brightness of the inner and outer rings further supports a collision origin. When a bar induces a strong pair of rings, the most prominent one is generally the inner, located just beyond the extremity of the bar at the so-called 4:1 resonance. In M 31, the outer ring is much brighter than the inner one. This makes the interpretation of bar-induced resonance rings highly unlikely except under the unrealistic hypothesis of a very slowly-rotating bar extending up to the outer ring (contrary to observations). The dual-ring morphology of M 31 strongly indicates expanding ringedensity waves triggered by a head-on galaxy collision with a companion.

The dwarf companion galaxy M 32 is very likely to be the impactor. To investigate whether a collision of M 32 with the disk of M 31 could induce the two-ringed density waves identified in the IRAC images, N-body simulations were performed<sup>21</sup>. The simulations include stars, gas, and dark matter in M 31 and M 32 with one million particles and a spatial resolution of 350 parsecs. Our simulations differ from all previous ones in that the initial orbit of M 32 is close to the polar axis of M 31, and the mass ratio is larger. Previous simulations<sup>5</sup> have assumed that the impact occurred several kiloparsecs away from the center of M 31 and not along the rotation axis (nearly head-on). Our new simulations start with an axisymmetric disk, proceed 1 Gyr while a bar and spiral arms form, then introduce a collision with M 32. We not only take into account the mass stripped during the collision but also take cognizance of the dark matter associated with M 32 itself. We assume an initial mass ratio for M 32 of 1/10 that of M 31 (including dark matter). Current-epoch mass estimates of M 32 are lower, but much mass is likely to have been stripped<sup>22</sup> during the collision. The final mass of M 32 in our model is 1/23 that of M 31, compatible with present-day mass estimates.

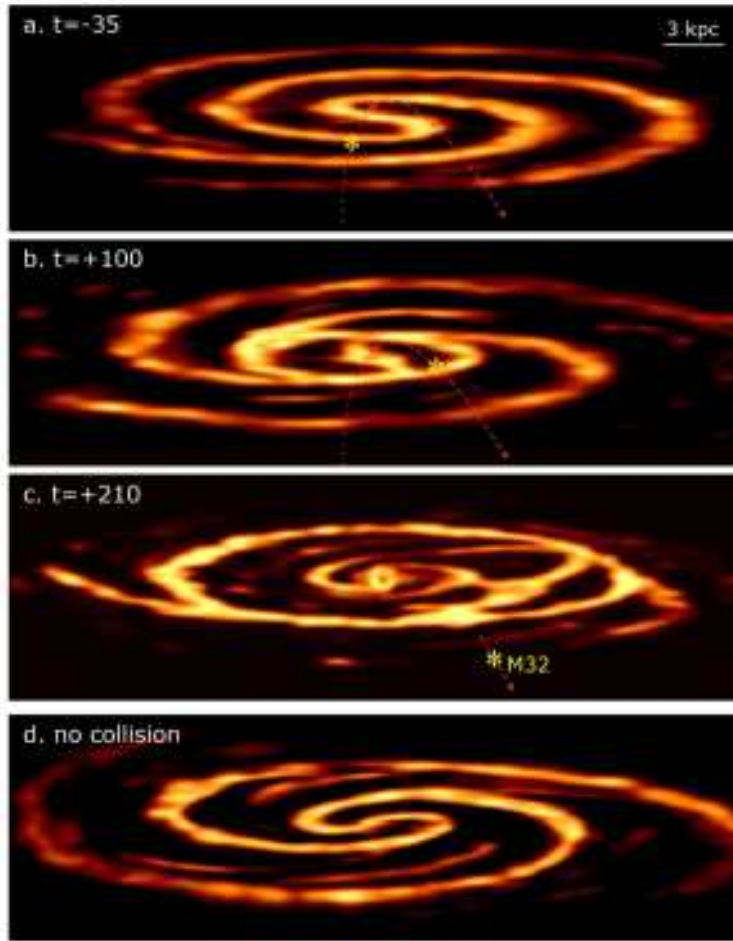


**Fig. 2.** Gas morphology produced by simulations<sup>21</sup> of a head-on encounter between M 31 and M 32. These N-body models include the gravitational dynamics of stars, interstellar matter, and dark matter in both M 31 and M 32. A "sticky-particle" scheme accounts for the dissipative nature of the interstellar medium, and star formation is also included<sup>21</sup>. The dashed red line demarcates the orbit of M 32; the locale of impact lies very close to the polar axis of M 31. Snapshots a, b, and c occur at  $t = 35$  million years (Myr) prior to collision and at 100 and 210 Myr post impact; the latter snapshot also shows the position of M 32 as we see it today. All snapshots are with the disk viewed at an inclination angle of 77 degrees for direct comparison with Figure 1. Snapshot c shows the central region of M 31 warped by a tilt angle of 30 degrees with respect to the main disk plane in accord with observations<sup>14</sup>. The two ring-like waves (both offset from the galaxy center) are seen, as is the hole in the outer ring. Snapshot d shows the gas morphology at  $t = 210$  Myr starting from the same initial disk conditions but modeled without a collision; no density-wave rings are generated. The initial mass ratio for the companion M 32 is 1/10th that of M 31 (or 1/13th excluding dark matter). The companion is assumed to impact the M 31 disk at a velocity of 265 km/s with an impact parameter of 4 kpc. It would now be located at a distance of 35 kpc and at a galactic latitude of about 45 degrees, which is fully compatible with the present position<sup>30</sup> of M 32.

The simulation of a head-on collision (Figure 2) beautifully reproduces the observed global morphologies of M 31 reported in this Letter. The model produces two striking density wave rings offset from the galaxy center. The outer density wave propagates through the M 31 disk, resulting in a perturbed interlacing of spiral features with an outer ring. This produces the conspicuous hole observed in the outer 10 kpc ring of M 31 (compare Figures 1 and 2). Our model reproduces this very striking (but transient) feature and adds compelling evidence that the two rings have been induced by a collision 210 million years ago close to the rotation axis of M 31. The non-zero (but small) impact parameter produces the off-center of the inner ring, and the inclination of the orbit with respect to the rotation axis produces the ring elongation. In the simulations, the head-on collision does not destroy the pre-existing boxy bulge in the barred target disk but merely weakens it.

Collisional ring galaxies are expected to show local radial and tangential perturbed motions in the vicinity of the rings, which will be observed as "streaming motions". When the intruder is one-fourth or less as massive as the disk

galaxy, the ring behaves like a wave which propagates through the disk<sup>23</sup>, as opposed to the large-scale bulk motion of material that occurs when the mass of the intruder is larger. Our model predicts radial velocities in the gas of 10 km/s at the outer (10 kpc) ring. Unwin<sup>24</sup> finds local streaming velocities in neutral hydrogen gas of 30 km/s at that radius; our predicted radial velocities constitute 30 percent of the total observed streaming velocity. The inner ring is predicted to show lesser radial velocities, which are more difficult to probe because of the vertical tilt of the central gas disk. There is an interesting kinematic signature of a ring induced by collision: the resulting positive radial velocity in the ring is predicted to be associated with a depression in the rotational velocity towards the outer parts of the ring (with a corresponding increase in the inner parts of the ring). This is indeed seen in most isovelocity contours in neutral hydrogen<sup>24</sup>. The predicted tangential streaming motions are actually opposite to the sense expected for spiral arm density waves<sup>25</sup>. Supplementary information is linked to the online version of the paper at [www.nature.com/nature](http://www.nature.com/nature) (See Appendix in this preprint).

The most striking analog of the disk morphology observed in M 31 is the Cartwheel Galaxy. The Cartwheel is the archetype of a double-ringed morphology produced by collision. Two distinct density wave rings are observed: a conspicuous outer ring, associated with massive star formation, and an elliptical inner ring, offset from the center of the galaxy. In between the two rings lie several spiral arms, termed spokes, which have developed in a trailing pattern. Several models have been computed of the Cartwheel Galaxy, simulating the almost head-on collision with one of its companions<sup>26,27</sup>.

M 31 contrasts with the Cartwheel Galaxy in that we do not see the inner ring in starlight but only in gas and dust. In other words, the inner ring in the Cartwheel Galaxy shows a much greater degree of contrast (compared to the parent disk) than does the inner ring in M 31. The explanation is that the impactor in the Cartwheel Galaxy must have been more massive than M 32, resulting in two density-wave rings of stars. Our simulations match the lower contrast seen in M 31: the primary ring wave propagates outward in the disk, being created by a crowding of particle trajectories and triggered massive star formation at the peak of the wave. The second elongated density-wave ring begins to propagate in the central regions of the galaxy, most likely in a tilted central disk. At the present epoch, the gas morphology of the model agrees with the double-ring structure of the M 31 interstellar medium as revealed by Spitzer/IRAC.

The peculiar morphology of M 31 has been mysterious for many years, but the discovery of the offset inner ring may be the clue needed to offer an explanation: a recent head-on collision can produce both the inner ring and the previously-known outer one. The rings are unlikely to have been created by bar resonances because of the rings relative brightness and their offsets from the galaxy center and also because they show no relationship to the spiral structure; in particular, no minor axis bar is observed. While head-on collisions between galaxies may have been common in the early Universe<sup>28,29</sup>, only a handful are known nearby. The discovery of one in our near neighbor M 31 affords the unique opportunity of studying such a collision at unprecedented spatial resolution.

### Appendix – Supplementary information: The velocity field and streaming motions induced by the head-on collision

Ring waves induced in a target galaxy disk by a head-on collision produce specific velocity perturbations, which may provide a signature of the event. Models show how complex these perturbations are when all three dimensions are taken into account<sup>17</sup>. In addition to the perturbation in the rotational (tangential) and radial velocities, there are characteristic velocities perpendicular to the disk plane, which becomes warped and corrugated. Fortunately, due to the high inclination of M 31, the velocity perturbations perpendicular to the plane will have little effect on the Doppler velocities observed from our direction.

For small perturbations, such as the one proposed here (where the companion mass is less than 1/10 of the target mass), it is possible to model the perturbation analytically with first order epicyclic theory: after receiving a velocity impulse due to the passage of the companion through the target galaxy, the particles in the target disk execute small oscillations around a guiding centre in a circular orbit. Most of the effect at the beginning of the perturbation can be modelled by the resulting kinematic wave, the self-gravity of the perturbation only becoming important at later epochs. The epicyclic approximation considers the induced oscillations to be harmonic, with a small variation  $\delta r$  in galactocentric radius:

$$r = r_0 + \delta r \cos \kappa t \quad (1)$$

and in azimuth

$$\Theta = \Omega t - 2\Omega/\kappa \delta r/r \sin \kappa t \quad (2)$$

The galactocentric radial velocity is then

$$V_r = -\kappa r \sin \kappa t \quad (3)$$

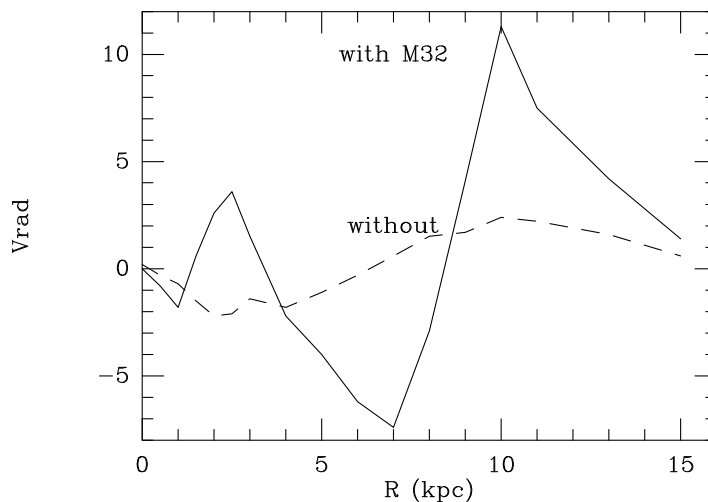


**Fig. 3.** Predicted ring-induced galactocentric radial velocities (averaged azimuthally) in our numerical model of M 31. The solid line shows radial velocities in our model after the collision with M 32. The dashed line shows the unperturbed disk of M 31 with only its underlying spiral structure.

and the perturbation in tangential velocity is

$$V_t = -2\Omega\delta r \cos \kappa t \quad (4)$$

( $\Omega$  and  $\kappa$  are the rotation and epicyclic angular frequencies, respectively).

At a particular epoch, an induced ring wave appears where particles expanding outwards in their epicycle oscillation encounter particles in other orbits flowing inward. The sense of the dominating radial velocity of most particles in the ring depends on the precise potential and variation of the epicyclic frequency  $\kappa$  with radius. For a flat rotation curve (as appropriate to M 31 at a radius of 10 kpc), the predicted radial velocity is positive. The magnitude of this radial velocity can be estimated from knowledge that  $\kappa$  is  $\simeq 1.4\Omega$  for a flat rotation curve. With a companion whose mass is 10% of the target disk mass, the maximum amplitude  $\delta r/r$  is 10% in the centre, where the companion impacts the disk. In the outer parts, where the outer ring is currently located, the amplitude should be less, of order 5%. The maximum radial velocity perturbation is then  $0.05 \times 1.4\Omega r$ , or equivalently  $0.07 V_{rot}$ , where  $V_{rot}$  is the rotational velocity. If  $V_{rot} = 200$  km/s, we expect a *maximum* radial velocity of 14 km/s. The observed velocity will be less because not all particles in the ring are in outward motion, and not all those are at their maximum velocity. Thus the radial kinematical effect one can realistically expect is 0.7 times the maximum or 10 km/s. The numerical model confirms this analytic estimate, as shown in Figure 3.

As noted in the previous paragraph, the epicyclic approximation predicts larger perturbations in the tangential velocities for a flat rotation curve by a factor of 1.4. In the numerical model, tangential streaming motions are indeed seen ranging between 15 and 20 km/s at the 10 kpc ring radius. The sense of the dominating velocities in the ring wave depends on the potential, and a gradient of velocity is predicted at the ring crossing. When the companion crosses the target disk, particles are given an inward pull, and the conservation of angular momentum requires that tangential velocities increase with respect to the circular velocity. When particles then expand outwards in their epicycle, their tangential velocity reaches a minimum at their apocenter. The kinematic signature of a resulting positive radial velocity in the ring will thus be associated with a decreased rotational velocity towards the outer parts of the ring and a corresponding increased rotational velocity in the inner parts of the ring. This signature is very significant: the predicted tangential streaming motions are actually opposite to the sense expected for spiral arm density waves. Spiral arms cause a tangential velocity increase just outside the arm and decrease on the inner side of the arm<sup>25</sup>.

Streaming motions are indeed observed in M 31 in both the neutral hydrogen gas<sup>24</sup> and in the CO-traced molecular component<sup>2,3</sup>. The streaming motions are more readily determined in the diffuse neutral component because the molecular gas is patchier. Only a moderate spatial resolution is necessary or even desirable because higher-resolution maps reveal motions on the scale where star formation perturbations (ionized gas expansion, supernovae driven bubbles, and the like) dominate.

In the observed Doppler velocities, the perturbations in the galactocentric radial and tangential directions are blended in various proportions, depending on the position of a given point with respect to the major or minor axis. On

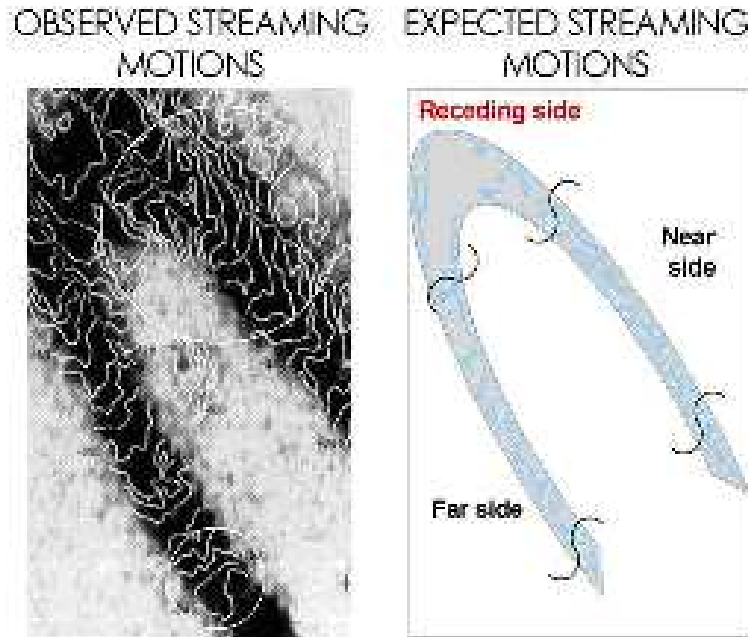


**Fig. 4.** IsovLOCITY curves observed in neutral hydrogen gas<sup>24</sup> compared with predictions from our collisional model. The contour interval is 10 km/s. The northern part of M 31 is the receding part (redshifted). The near side is NW and the far side SE. The expected wiggles are indicated for the regions near the minor axis (radial velocity outwards for the outer part of the ring) and for the regions near the major axis (depression of tangential velocity in the outer part of the ring). The "S" curves schematically depict expected Doppler velocities; only the portion within the ring area (shaded blue) can be observed. The regions where the streaming motions support the collisional model are circled in white.

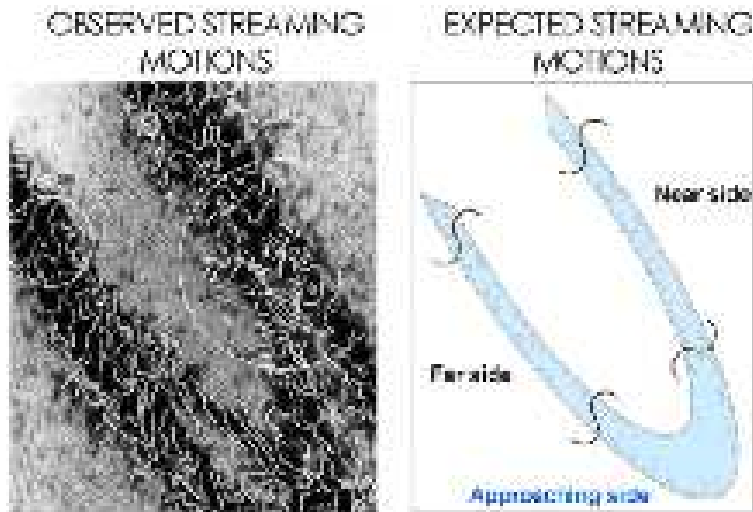


**Fig. 5.** Same as for supplementary Fig. 4, but for the southern sector of M 31, which is approaching the observer (blue-shifted).

the major axis only tangential velocities are measured; on the minor axis, only radial. The inclination of M 31 is large enough that it can be considered nearly edge-on, but this same high inclination of M 31 makes it difficult to disentangle the radial velocity components of the rings and spiral arms because both are squeezed in projection along the minor axis. Near the major axis, though, where tangential perturbations are expected to dominate, projection is less of a problem. The observed isovelocity curves (see figures 4 and 5) in fact show wiggles around the 10 kpc ring radius. The sense of these wiggles favours a depression of tangential velocity in the outer parts of the arm/ring. This favours our interpretation in terms of a ring induced by collision rather than spiral density waves. In other sectors of the galaxy, the streaming motions correspond to density-wave features, as expected from the underlying spiral structure.

*Acknowledgements.* This work is based on observations made with the Spitzer Space Telescope, which is operated by the Jet Propulsion Laboratory, California Institute of Technology under a contract with NASA. Funding for this work was provided by the Anglo American Chairmans Fund as well as by NASA through an award issued by JPL/Caltech.

P.B., G.F., M.A., M.P. and S.W. provided the Spitzer-IRAC data of M31 on which the analyses are based. D.L.B. initiated the collaboration between the U.S.A, France and South Africa and identified Baade dust spirals in emission in the central region of M31. F.C. discovered the central ring between the inner Baade arms and believed it to be induced by a head-on collision. F.B. performed the numerical simulations which fully corroborated this interpretation and also generated Figures 1 and 2. R.G. cleaned the IRAC images of foreground stars and conducted Fourier spectral analysis of the Baade arms. F.C. and F.B. provided crucial drafts of this Letter. The final revised versions were prepared by D.L.B., S.W, R.G. and M.A.

## References

1. Brinks E. & Shane W.W., *Astron. Astrophys. Suppl.* 55, 179-251 (1984).
2. Dame, T.M., Koper, E., Israel, F. P. & Thaddeus, P. , *Astrophys. J.* 418, 730-742 (1993).
3. Nieten, C. et al., *Astron. Astrophys.*, 453, 459-475 (2006).
4. Haas, M., Lemke, D., Stickel, M., Hippelein, H., Kunkel, M., Herbstmeier, U. & Mattila, *Astron. Astrophys.* 338, L33-36 (1998).
5. Gordon, K.D. et al., *Astrophys. J.*, 638, L87-L92 (2006).
6. Beck, R., Berkhuijsen, E.M. & Hoernes, P., *Astron. Astrophys. Suppl.* 129, 329-336 (1998).
7. Pellet, A., Astier, N., Viale, A., Courtes, G., Maucherat, A., Monnet, G. & Simien, F., *Astron. Astrophys. Suppl.* 31, 439-461 (1978).
8. Ibata, R. et al., *Nature* 412, 49-51 (2001).
9. Braun, R., *Astrophys. J.* 372, 54-66 (1991).
10. Barmby, P. et al., M 31. *Astrophys. J.* 650, L45 (2006).
11. Fazio, G.G. et al., *Astrophys. J. Suppl.* 154, 10-17 (2004).
12. Stanek, K. Z. and Garnavich, P. M., *Astrophys. J.* 503, L131-134 (1998)
13. Baade, W. *Evolution of stars and galaxies.* Cambridge, Harvard University Press, (1963).
14. Jacoby, G.H., Ford, H. & Ciardullo, R., *Astrophys. J.* 290, 136-139 (1985).
15. Willaime, M-C., Lequeux, J., Melchior, A-L. & Hanus, M. in *The Promise of the Herschel Space Observatory.* Eds. G.L. Pilbratt, et al. ESA-SP 460, 519-521 (2001).
16. Ciardullo, R. et al., *Astron. J.* 95, 438-444 (1998).
17. Appleton, P.N. & Struck-Marcell, C., *Collisional Ring Galaxies, Fundamentals of Cosmic Physics*, 16, 111-220 (1996).
18. Buta, R., *Astrophys. J. Suppl.*, 96, 39-116 (1995).
19. Block, D.L., Puerari, I., Knapen, J.H., Elmegreen, B.G., Buta, R., Stedman, S. & Elmegreen, D. M., *Astron. Astrophys.* 375, 761-769 (2001).
20. Beaton, R.L., Majewski, S.R., Guhathakurta, P., Strutskie, M.F., Cutri, R.M., Good, J., Patterson, R.J., Athanassoula, E., Bureau, M., *Astrophys. J.*, submitted (2006) astro-ph/0605239.
21. Bournaud, F. & Combes, F., *Astron. Astrophys.* 401, 817-833 (2003).
22. Welch, G.A. & Sage, L.J., *Astrophys. J.*, 557, 671-680, (2000).
23. Gerber, R.A., Lamb, S.A. & Balsara, D.S., *Mon. Not. R. Astron. Soc.* 278, 345-366 (1996).
24. Unwin, S.C., *Mon. Not. R. Astron. Soc.* 205, 773-786 (1983).
25. Shu, F.H., Milione, V. & Roberts, W.W., *Astrophys. J.* 183, 819-842 (1973).
26. Struck-Marcell, C. & Higdon, J.L., *Astrophys. J.* 411, 108-124 (1993).
27. Horellou, C. & Combes, F., *Astrophys. & Space Sci.* 276, 1141-1149 (2001).
28. Lavery, R.J., Remijan, A., Charmandaris, V., Hayes, R.D. & Ring, A.A., *Astrophys. J.* 612, Issue 2, 679-689 (2004).
29. Elmegreen, D.M., Elmegreen, B.G., Rubin, D.S. & Schaffer, M.A., *Astrophys. J.* 631, 85-100 (2005).
30. Mateo, M., *Ann. Rev. Astron. Astrophys.* 36, 435-506 (1998).